A low complexity representation of the coherent point spread function in the presence of aberrations and arbitrarily large defocus

by

Saeed Bagheri

Submitted to the Department of Mechanical Engineering
in partial fulfillment of the requirements for the degree of

Master of Science in Mechanical Engineering

at the

MASSACHUSETTS INSTITUTE OF TECHNOLOGY

January 2006
[February 2006]

Author .....
Department of Mechanical Engineering
January 10, 2006

Certified by .....
Daniela Pucci de Farias
Assistant Professor, Mechanical Engineering
Thesis Supervisor

Accepted by .....
Lallit Anand
Chairman, Department Committee on Graduate Students

A low complexity representation of the coherent point spread function in the presence of aberrations and arbitrarily large defocus

by

Saeed Bagheri

Submitted to the Department of Mechanical Engineering
on January 10, 2006, in partial fulfillment of the
requirements for the degree of
Master of Science in Mechanical Engineering

Abstract

In this thesis we introduce a new method for analyzing the diffraction integral for evaluating the point spread function. The new method is based on the use of *higher order Airy functions* along with Zernike and Taylor expansions. Our approach is applicable when we are considering a finite, arbitrary number of aberrations and arbitrary large defocus simultaneously. We present an upper bound for the complexity and the convergence rate of this method. We also compare the cost and accuracy of this method to traditional ones and show the efficiency of our method through these comparisons. In particular, we rigorously show that this method is constructed in a way that the complexity of the analysis (i.e the number of terms needed for expressing the light disturbance) does not increase as either of defocus or resolution of interest increases. This has applications in several fields such as biological microscopy, lithography and multi-domain optimization in optical systems.

Thesis Supervisor: Daniela Pucci de Farias
Title: Assistant Professor, Mechanical Engineering

Contents

List of Figures

Chapter 1

Introduction

1.1 Motivation

The importance of studying the effects of aberrations and defocus on the basis of diffraction theory is very well understood [2] and recent new applications of it, such as biological microscopy [8], lithography [13] and multi-domain optimization techniques in optical systems [6, 11], which need high resolution and accurate value of the point spread function, have called for a more comprehensive study. For instance, recent articles have reported the use of intentionally adding aberrations for making more sophisticated optical systems. [6] Further steps in this direction require a more involved analysis of the diffraction integral in the presence of aberrations and defocus, in order to simplify the process of evaluating the point spread function.

1.2 Background

Solving the diffraction integral to find an analytical form for the field distribution on the image plane depends crucially on the defocus and aberration factors. The original Nijboer-Zernike approach for this purpose can only lead to a reasonable approximation when the wavefront deviation due to aberrations and defocus remains within a few radians. [9, 2] Also, even when aberrations and defocus factors are small, but many of them coexist, the Nijboer-Zernike method becomes too cumbersome to follow. [9]

Recently, extensions of the original Nijboer-Zernike method have been developed in order to make it applicable to larger values of defocus and aberrations. Nevertheless the basis for all of those methods is the same as the original Nijboer-Zernike method and some of the limitations of the original method still apply to all of the newly developed versions. For instance, by considering more than one aberration term (apart from defocus) the number of terms necessary for the diffraction integral and the calculation involved increase significantly. [3, 9, 4]

1.3 Our Approach

We present a new method for attacking the diffraction integral problem. Our main result is the following expansion for the point spread function h:

$$h(x, y; x_0, y_0) = \sum_{n,m} A'_{nm} \frac{J_{n+1}(R)}{R} \cos[m(\Theta + \phi_0)],$$

where $J_{n+1}(R)$ is the $(n+1)^{\text{th}}$ order first kind Bessel function, (x, y) and (x_0, y_0) are Cartesian coordinate systems at the image and object planes respectively, $R\angle\Theta$ is a polar coordinate system related to those two coordinate systems and $r_0\angle\phi_0$ is the polar coordinate system in the object plane. The coefficients A'_{nm} are polynomials of the aberration constants and of the defocus coefficient multiplied by a factor that is exponential on the defocus coefficient. Functions $\frac{J_n(R)}{R}$ used in the expansion are denoted as *higher order Airy functions.* Our method for developing the above representation for h is novel and requires a sequence of Taylor and Zernike expansions. The expansions are combined so as to capture the physics of diffraction with a circular aperture.

Our expansion for the point spread function exhibits several desirable properties. It can be used to evaluate the point spread function for systems with an arbitrary number of aberrations. It is also computationally tractable and numerically stable over all ranges of defocus values. By taking advantage of the closed-form solution, the diffraction integral may be evaluated within any arbitrary resolution using our expansion. We show that, even though exact representation of h involves an infinite summation of polynomials A'_{nm} of infinite degree, the number of terms and polynomial degree required to achieve a prescribed accuracy, scale gracefully with the system parameters. Specifically, we establish an explicit bound showing that, in order to achieve an accuracy of ϵ, the required number of terms grows linearly with the values of aberrations (excluding defocus), the maximum value of R of interest and $\log\frac{1}{\epsilon}$, and is independent of the remaining parameters of the system (including defocus). Furthermore, numerical experiments show that the bound is loose and in practice

even fewer terms may suffice. This means that unlike previous methods [3, 9, 4], the complexity of our expansion does not increase as either of defocus or resolution of interest increases.

In the next chapter we formally state the problem; this includes the basic assumptions for deriving the diffraction integral and the general aberration form. In chapter 3, we present the main result which is the general form for the point spread function. There, we consider the most general representation for aberration functions and defocus. We also analyze the general result when all primary aberrations and defocus are simultaneously present. In this chapter, we also present some examples of point spread function in the case of primary aberrations. In chapter 4, we analyze the complexity of our method. We present an upper bound for the number of terms and degree of polynomials required in the expansion of h in order to achieve a prescribed accuracy. In chapter 5, we compare the cost and accuracy of this method to traditional ones and show the efficiency of our method through these comparisons. We conclude in chapter 6.

Chapter 2

The Optical Point Spread Function

2.1 Introduction

In this chapter, we introduce the point spread function (PSF). Figure 2-1 shows the configuration of an arbitrary optical system in the object plane, image plane and pupil plane for computing the PSF. We assume that the usual Sommerfeld-Kirchhoff assumptions hold, and that the chromatic aberrations are negligible. The PSF h is used to calculate the image disturbance $\vec{Q}$ caused by a monochromatic coherent plane wave illumination in an arbitrary plane parallel to the exit pupil in the presence of an object $\vec{P}$. In particular, at each point (x, y) on the image plane, we have

$$\vec{Q}(x,y) = \int_{\mathcal{A}} h(x,y;x_0,y_0)\,\vec{P}(x_0,y_0)\,dx_0\,dy_0, \tag{2.1}$$

where $\mathcal{A}$ is the whole object domain in the object plane.

The PSF h can be further specified as follows: Consider a point source of mono-

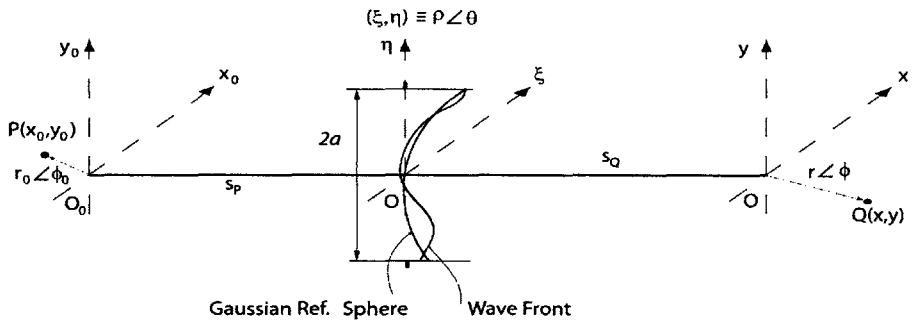

Figure 2-1: Schematic view of the optical system under consideration.

chromatic light P and find the disturbance in an arbitrary point Q in space, assuming a circular aperture of radius a. Let (x_0, y_0) denote the ray entrance Cartesian coordinates on the object plane at distance S_P from the entrance pupil and let $r_0\angle\phi_0$ represent the respective polar coordinates. According to Huygens-Fresnel principle, the disturbance at an arbitrary point (x, y) (or in polar coordinates $r\angle\phi$) on the image plane at distance S_Q from the exit pupil is

$$h(x, y; x_0, y_0) = C \int_0^1 \int_0^{2\pi} \mathrm{e}^{\mathrm{i}\, k\, w(\rho,\theta,r_0,\phi_0)} \mathrm{e}^{\mathrm{i}R\rho\cos(\theta-\Theta)} \rho\, d\rho\, d\theta. \tag{2.2}$$

The image plane is not necessarily the Gaussian image plane, which is at distance S_G of the lens. In this formulation, ρ and θ, which are integral variables, are polar coordinates in the exit pupil plane. Coordinates R and Θ are polar equivalents of the point (u, v), which is related to (x_0, y_0) and (x, y) according to

$$u = -k\, a \left(\frac{x_0}{r'} + \frac{x}{s'}\right), \tag{2.3}$$

$$v = -k\, a \left(\frac{y_0}{r'} + \frac{y}{s'}\right), \tag{2.4}$$

$$r'^2 = {x_0}^2 + {y_0}^2 + {S_P}^2, \tag{2.5}$$

$$s'^2 = x^2 + y^2 + {S_Q}^2, \tag{2.6}$$

where $k = 2\pi/\lambda$ is the wave number. The wavefront error w includes all aberrations and defocus terms.

2.2 The Wavefront Error

According to Schwarzschild's Analysis [5], we have

$$w(\rho, \theta, r_0, \phi_0) = \sum_{j=1}^{n_{ab}} \left\{ f_{L_j,M_j}({r_0}^2)\,(a\,\rho)^{2L_j}\ [a\,\rho\,\cos(\theta - \phi_0)]^{M_j} \right\}, \tag{2.7}$$

$$f_{L_1,M_1} = f_{1,0} = DF = \frac{1}{2}\left(\frac{1}{S_Q} - \frac{1}{S_G}\right). \tag{2.8}$$

In Eq. (7), n_{ab} is the total number of aberrations under consideration. Note that the particular value of L_j and M_j identifies the type of aberration which j is referring to. In particular $f_{1,0}$ or DF is referred to as the defocus coefficient. We treat defocus separately in order to make the complexity of the expansion independent of defocus. Also note that w is the deviation of the wavefront from the Gaussian reference sphere in the exit pupil. In terms of optical path lengths, w is a function of the source coordinate and coordinates of the exit pupil. $f_{L,M}$ are referred to as the aberration coefficients.

2.3 The Normalized Point Spread Function

It can be shown that the coefficient C in Eq. (2.2) is [2]

$$C = \frac{\mathbf{i}\, k \cos(\delta)}{2\pi r' s'}. \tag{2.9}$$

with δ defined as the acute angle which satisfies

$$tan(\delta) = \frac{\sqrt{(x_0 + x)^2 + (y_0 + y)^2}}{z_0 + z}. \tag{2.10}$$

Note that C is bounded in the whole region of integration as

$$|C| \leq \frac{k}{2\pi |S_P||S_Q|}. \tag{2.11}$$

Thus, to attack the main problem of finding an analytic solution to the diffraction integral, we may neglect the coefficient C in Eq. (2.2), and define $\hat{h}$, the normalized PSF, as

$$\hat{h}(x, y; x_0, y_0) = \frac{1}{2\pi} \int_0^1 \int_0^{2\pi} \mathrm{e}^{\mathbf{i}\, k\, w(\rho,\theta,r_0,\phi_0)} \mathrm{e}^{\mathbf{i} R\rho \cos(\theta - \Theta)} \rho \, d\rho \, d\theta. \tag{2.12}$$

In this thesis we develop an expansion for $\hat{h}$ in terms of polynomials, in the presence of aberrations and defocus. The expansion involves an infinite sum of polynomials, but we show that, for any given accuracy, only a finite number of terms is required.

Chapter 3

Main Result

3.1 The Point Spread Function Expansion for Arbitrary Wavefront Errors and Defocus

We now present a general expression for the PSF as an expansion in terms of *higher order Airy functions*. We define the n^{th} order Airy function as

$$n^{th}\,\text{orderAiryfunction} = \frac{J_{n+1}(R)}{R},$$

where J_{n+1} is the $(n+1)^{\text{th}}$ order first kind Bessel function.

We represent the PSF as a sum of polynomials of the aberration and defocus coefficients. In this chapter, finitely many of the aberration terms in Schwarzschild's analysis are considered. In practice, however, only a few of those (usually the primary aberrations) are of real importance. We illustrate application of our result in one such

case in the next section.

Our proposed expansion is of the form

$$\hat{h}(x,y;x_0,y_0) = \sum_{n=0}^{\infty}\sum_{m=0}^{n}\left\{\tilde{\delta}_{n-m}\delta_m A_{nm}\cos\left[m(\Theta+\phi_0)\right]\frac{J_{n+1}(R)}{R}\right\}, \tag{3.1}$$

where $\tilde{\delta}_i$, δ_i and the coefficients A_{nm} are given by Eqs. (3.2), (3.3) and (3.4) respectively.

$$\tilde{\delta}_i = \begin{cases} 1 & \text{if } i \text{ is even,} \\ 0 & \text{otherwise.} \end{cases} \tag{3.2}$$

$$\delta_i = \begin{cases} 1 & \text{if } i = 0, \\ 2 & \text{otherwise.} \end{cases} \tag{3.3}$$

$$A_{nm} = \frac{n+1}{2^{m-1}}\,\mathrm{e}^{\mathrm{i}\,m\phi_0}\sum_{(\mathbf{N},D)\in\aleph_m} D\,\beta_{\mathbf{N}}\,S^m_{n,k_{\mathbf{N}}}(\vec{\beta}). \tag{3.4}$$

$\aleph_m$ is a set of pairs of $n_{ab}-1$ element vectors $\mathbf{N} = [N_2,\ N_3,\ \ldots\ N_{n_{ab}}]$ and scalars D defined as

$$\aleph_m = \left\{(\mathbf{N},D)\ \Big|\ \sum_{j=2}^{n_{ab}}(M_jN_j) = m+2k,\ D = \frac{(m+2k)!}{2^{2k}k!(m+k)!};\ k, N_j \in \mathcal{N}\right\}. \tag{3.5}$$

where M_j is the proper parameter used in the definition of the j^{th} aberration as in Eq. (2.7). Function $S^m_{n,k_{\mathbf{N}}}(\vec{\beta})$ is given by

$$S^m_{n,k_{\mathbf{N}}}(\vec{\beta}) = \int_0^1 \prod_{j\in\chi_1} \mathrm{e}^{\beta_j \rho^{2L_j}}\, R^m_n(\rho)\, \rho^{k_{\mathbf{N}}+1}\, d\rho, \tag{3.6}$$

where $R^m_n(\rho)$ is the Zernike polynomial introduced in Appendix B, and we have

$$\beta_j = \mathbf{i}\, k\, f_{L_j,M_j}({r_0}^2)\, a^{2L_j+M_j}, \tag{3.7}$$

$$\beta_{\mathbf{N}} = \prod_{j\in\chi_2} \frac{(\beta_j)^{N_j}}{N_j!}, \tag{3.8}$$

$$k_{\mathbf{N}} = \sum_{j\in\chi_2} (2L_j + M_j)N_j, \tag{3.9}$$

$$\chi_1 = \{j \mid M_j = 0,\ j = 1,\ldots,n_{ab}\}, \tag{3.10}$$

$$\chi_2 = \{j \mid M_j \neq 0,\ j = 1,\ldots,n_{ab}\}, \tag{3.11}$$

$$\chi_3 = \{j \mid M_j = 0,\ j = 2,\ldots,n_{ab}\}. \tag{3.12}$$

A derivation of the expressions above can be found in Appendix B. Note that $S^m_{n,k_{\mathbf{N}}}(\vec{\beta})$ is defined implicitly in Eq. (3.6), requiring computation of an integral. An

explicit expression for the integral, which is based on a Taylor expansion of $e^{\beta_j \rho^{2L_j}}$ ($j \in \chi_3$), can be found in Appendix C. The derivation is tedious but relatively straightforward. It follows from this expansion that $S^m_{n,k_N}(\vec{\beta})$ can be expressed as a polynomial of aberration constants $\vec{\beta}$ multiplied by a factor that is exponential on the defocus coefficient.

The number of terms in the summation in Eq. (3.1) and the degree of the polynomials used to express $S^m_{n,k_N}(\vec{\beta})$ are infinite. However, in chapter 4 we show that, for any desired accuracy ϵ, a finite truncation of Eq. (3.1) as well as finite-degree polynomials for A_{nm} in Eq. (3.4) suffice for an appropriate approximation to h; i.e. Eq. (3.1) converges to Eq. (2.12). We give an explicit bound on the number of terms and degree required and show that they scale gracefully with the systems parameters and ϵ. This will be realized by giving an upper bound for n in Eq. (3.1) as well as an upper bound for every N_j in Eq. (3.5). Note that a bound on N_j will determine the number of terms of Taylor expansion of $e^{\beta_j \rho^{2L_j} [\cos(\theta - \phi_0)]^{M_j}}$ which have been used in our expansion.

In the next section we illustrate some of the applications of this expansion through examples.

3.2 Examples

In this section we consider the primary (Seidal) aberrations and defocus ($n_{ab} = 5$)

$$\mathbf{i}\,k\,(a)^{2L+M}\,f_{L,M}(r_0{}^2) = \begin{cases} \gamma_1 & \text{if (L,M)=(1,0) } \textit{Defocus and Field Curvature,} \\ \gamma_2 & \text{if (L,M)=(2,0) } \textit{Spherical Aberration,} \\ \gamma_3 & \text{if (L,M)=(0,1) } \textit{Distortion,} \\ \gamma_4 & \text{if (L,M)=(0,2) } \textit{Astigmatism,} \\ \gamma_5 & \text{if (L,M)=(1,1) } \textit{Coma,} \end{cases} \tag{3.13}$$

where for simplicity (x_0, y_0) is assumed to be $(0, 0)$. Substituting in Eq. (3.4) we have

$$\begin{aligned} A_{nm} &= \frac{n+1}{2^{m-1}}\,\mathbf{i}^{\,n} \times \\ &\sum_{(\mathbf{N},D)\in\aleph_m} D\left[\frac{\gamma_3^{N_3}\gamma_4^{N_4}\gamma_5^{N_5}}{N_3!N_4!N_5!}\,S^m_{n,N_3+2N_4+3N_5}(\gamma_1,\gamma_2)\right], \end{aligned} \tag{3.14}$$

where

$$\begin{aligned} \aleph_m &= \{(\mathbf{N}, D) = (N_3, N_4, N_5, D)\,| \\ &N_3 + 2N_4 + N_5 = m + 2k,\ D = \frac{(m+2k)!}{2^{2k}k!(m+k)!};\ k, N_3, N_4, N_5 \in \mathcal{N}\Big\}, \end{aligned} \tag{3.15}$$

$$S^m_{n,N_3+2N_4+3N_5}(\gamma_1,\gamma_2) = \int_0^1 \mathrm{e}^{\gamma_1\rho^2+\gamma_2\rho^4}\,R^m_n(\rho)\,\rho^{N_3+2N_4+3N_5+1}\,d\rho, \tag{3.16}$$

and the derivation of S can be found in Appendix C. So A_{nm} is a polynomial of γ_1, $\ldots$, γ_5. It also has one term in the form of $\exp(\gamma_1)$. Although from the above equation it seems that the order of this polynomial is infinity, as will be explained later, once

we set a target accuracy, all except for a few terms in A_{nm} become negligible. As it will be shown in chapter 4, the number of necessary terms in expression (3.14), scales favorably with the desired accuracy of the representation.

Now to evaluate the transfer function, $\hat{h}$, we can rewrite Eq. (3.1) as

$$\hat{h}(r\angle\phi) = \sum_{n=0}^{\infty}\sum_{m=0}^{n}\left\{\tilde{\delta}_{n-m}\delta_m A_{nm}\cos[m(\phi+\pi)]\frac{J_{n+1}(Br)}{Br}\right\}, \tag{3.17}$$

where $B = \frac{ka}{s}$ is obtained using Eqs. (2.3) and (2.4) and by setting (x_0, y_0) equal to $(0,0)$. As an example, the results using this method are shown in Fig. 3-1 for $Br < 20$. γ_2 and γ_3 are zero in this figure.

Thus, we have (note that since $\gamma_3 = 0$, $(\mathbf{N}, D)$ is a three element vector)

$$\begin{aligned}
\aleph_0 &= \Big\{(0,0,1),\ (2,0,\tfrac{1}{2}),\ (0,1,\tfrac{1}{2}),\ (4,0,\tfrac{3}{8}),\ (2,1,\tfrac{3}{8}),\ (0,2,\tfrac{3}{8}), \\
&\quad (4,1,\tfrac{5}{16}),\ (2,2,\tfrac{5}{16}),\ (0,3,\tfrac{5}{16}),\ (4,2,\tfrac{35}{128}),\ (2,3,\tfrac{35}{128}), \\
&\quad (0,4,\tfrac{35}{128}),\ (4,3,\tfrac{63}{256}),\ (2,4,\tfrac{63}{256}),\ (4,4,\tfrac{231}{1024})\Big\}, \\
&\quad \vdots \\
\aleph_{11} &= \{(3,4,1)\}, \\
\aleph_{12} &= \{(4,4,1)\},
\end{aligned} \tag{3.18}$$

and $\aleph_m = \{\}$ otherwise. This means that A_{nm} is zero for $m > 12$. Also in this special case, Eq. (3.16) reduces to

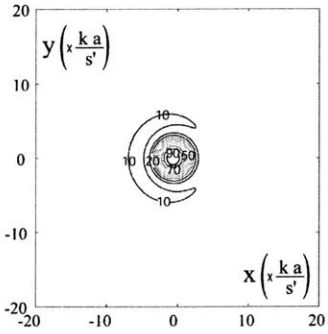

(a) $\gamma_1 = 0$, $\gamma_4 = 0$, $\gamma_5 = 1\mathbf{i}$.

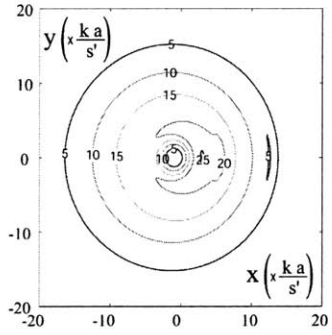

(b) $\gamma_1 = 2\pi\mathbf{i}$, $\gamma_4 = 0$, $\gamma_5 = 1\mathbf{i}$.

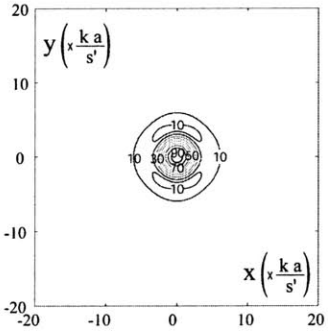

(c) $\gamma_1 = 0$, $\gamma_4 = 1\mathbf{i}$, $\gamma_5 = 0$.

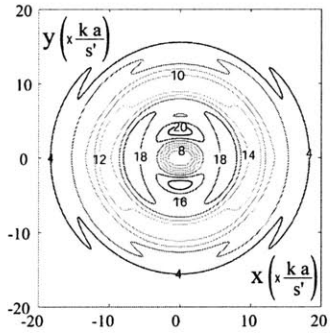

(d) $\gamma_1 = 2\pi\mathbf{i}$, $\gamma_4 = 1\mathbf{i}$, $\gamma_5 = 0$.

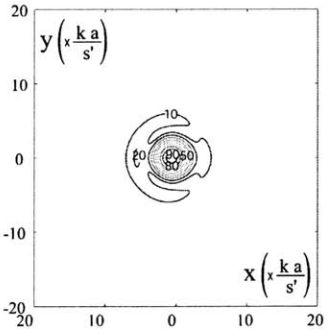

(e) $\gamma_1 = 0$, $\gamma_4 = 1\mathbf{i}$, $\gamma_5 = 1\mathbf{i}$.

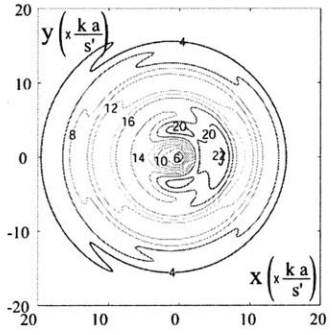

(f) $\gamma_1 = 2\pi\mathbf{i}$, $\gamma_4 = 1\mathbf{i}$, $\gamma_5 = 1\mathbf{i}$.

Figure 3-1: Contour plot of modulus of the PSF, $|h|$, in the presence of aberrations and defocus (normalized to 100).

$$S^m_{n,k'}(\gamma_1) = \sum_{l=0}^{(n-m)/2} \left(\frac{C^m_{n,l}}{2} (-\gamma_1)^{\frac{-(2+n-2l+k')}{2}} (\frac{n-2l+k'}{2})! \left[1 - \mathrm{e}^{\gamma_1} \sum_{j=0}^{\frac{n-2l+k'}{2}} \frac{(-\gamma_1)^j}{j!} \right] \right), \tag{3.19}$$

where $C^m_{n,l}$ is defined in Eq. (B.3).

Chapter 4

Complexity Analysis

4.1 Introduction

In this chapter we analyze the complexity of our representation of the PSF. Specifically, we show rigorously that within a confined region of space (i.e. the exit window) the PSF can be expressed within any arbitrary accuracy, using a finite number of terms in Eq. (3.1) regardless of the value of defocus and desired resolution (Note that by resolution, we mean the shortest distance between two points where we are interested to evaluate PSF). This means that, as we increase the resolution of interest or as we change the defocus, the number of necessary terms within the prescribed accuracy do not change. This is of great importance in many practical cases where numerical simulation fails to generate the point spread function within the required resolution and accuracy in a reasonable time. This issue is revisited in the next chapter.

Considering a desired accuracy, the complexity of the expansion in Eq. (3.1) depends on three factors: (i) The maximum index of summation, n^*, considered in

Eq. (3.1). (ii) The number, N^*, of terms in the summation considered in Eq. (3.1); this number is $O\left((n^*)^2\right)$. (iii) The degree of polynomials involved in the expressions of A_{nm} in Eq. (3.1). These polynomials are at most on the order of ${N_j}^*$ on β_j, the j^{th} aberration coefficient, when $N_j \leq {N_j}^*$ in Eq. (3.5). We analyze all these three factors.

4.2 Statement of the Complexity

With the finite summation bound n^*, and the finite polynomial order ${N_j}^*$ for each aberration coefficient β_j, $j = 2, \ldots, n_{ab}$, Eq. (3.1) is rewritten as

$$\hat{h}_{n^*}(x, y; x_0, y_0) = \sum_{n=0}^{n^*} \sum_{m=0}^{n} \tilde{\delta}_{n-m} \delta_m A^*_{nm} \cos[(\Theta + \phi_0)] \frac{J_{n+1}(R)}{R}, \tag{4.1}$$

where A^*_{nm} is defined as

$$A^*_{nm} = \frac{n+1}{2^{m-1}} e^{im\phi_0} \sum_{(\mathbf{N}, D) \in \aleph^*_m} D\, \beta_{\mathbf{N}}\, S^m_{n,k_{\mathbf{N}}}(\vec{\beta})^*, \tag{4.2}$$

and $\aleph^*_m$ and $S^m_{n,k_{\mathbf{N}}}(\vec{\beta})^*$ are defined as

$$\aleph^*_m = \left\{ (\mathbf{N}, D) \mid \sum_{j=2}^{n_{ab}} (M_j N_j) = m + 2k,\ D = \frac{(m+2k)!}{2^{2k} k! (m+k)!};\ N_j \leq N^*_j,\ k, N_j \in \mathcal{N} \right\}, \tag{4.3}$$

$$S^m_{n,k_{\mathbf{N}}}(\vec{\beta})^* = \sum_{l=0}^{(n-m)/2} C^m_{n,l} \int_0^1 \mathrm{e}^{\beta_1 \rho^2} \prod_{j \in \chi_3} \left[\sum_{N_j=0}^{N_j^*} \frac{(\beta_j \rho^{2L_j})^{N_j}}{N_j!} \right] \rho^{n-2l+k_{\mathbf{N}}+1} \, d\rho. \tag{4.4}$$

Note that the only difference in the definition of $\aleph^*_m$ and $S^m_{n,k_{\mathbf{N}}}(\vec{\beta})^*$ and $\aleph_m$ and $S^m_{n,k_{\mathbf{N}}}(\vec{\beta})$ is that N_j is bounded by N_j^* in $\aleph^*_m$ and $S^m_{n,k_{\mathbf{N}}}(\vec{\beta})^*$.

As the accuracy of interest in Eq. (4.1) increases, the upper bounds for n and N_j, i.e. n^* and N_j^*, should also increase too. The change of these bounds as the desired accuracy in Eq. (4.1) changes, is an expression of complexity of our expansion. Theorem 4.2.1 provides us with such an expression, and is our main result in this chapter.

Theorem 4.2.1. *Let ϵ, n_{ab} and R^* be arbitrary and let*

$$n^* \geq \max\left(5,\, \mathrm{e}R^* + 1,\, 2\log_2 \frac{1}{\mathrm{e}(2\mathrm{e}-1)\sqrt{\pi}\epsilon}\right),$$

and

$$N_j{}^* \geq \max\left(4,\, 2\mathrm{e}\,|\beta_j| + 1,\, \log_2 \frac{\sqrt{6\mathrm{e}}\,\mathrm{e}^3\, n_{ab}\,(1 + R^{*4/3})}{\pi(2\mathrm{e}-1)\epsilon}\right),$$

for all $j = 2, \ldots, n_{ab}$. Then we have

$$|\hat{h}(x, y; x_0, y_0) - \hat{h}_{n^*}(x, y; x_0, y_0)| \leq \epsilon$$

for all x, y, x_0, y_0 such that the corresponding value of R is less than or equal to R^*.

Theorem 4.2.1 provides us with an upper bound to the minimum necessary index of summation in Eqs. (4.1) and (4.2) and proves that it is finite. In fact, numerical simulations in practice suggest that even smaller minimum necessary indices of summation would suffice. A proof of Theorem (4.2.1) can be found in Appendix D.

Thus, we have shown that any arbitrary accuracy of the light disturbance in the circle of $R \leq R^*$ can be achieved with a sufficiently large finite value of n^* and N_j^*s. Theorem 4.2.1 states that as the radius of the region of interest, R^*, increases, the maximum necessary index of summation in Eq. (4.1), n^*, increases linearly with R^*. It also indicates that the maximum necessary index of summation in Eq. (4.1), n^*, increases proportionally to $\log \frac{1}{\epsilon}$, where ϵ is the accuracy of approximation. We can also see that the maximum necessary index of summation in Eq. (4.2) (as stated in Eqs. (4.3) and (4.4)), N_j^*, or in other words, the maximum order of β_j in the expression of A_{nm}s, increases linearly with the corresponding aberration coefficient $|\beta_j|$ and $\log \frac{1}{\epsilon}$, where ϵ is the accuracy of approximation. The $\log \frac{1}{\epsilon}$ dependence of n^* and N_j^* on the accuracy (ϵ) confirms the fast convergence of this method.

Considering the above analysis, we conclude that when we are interested in the disturbance in a confined region, we only need to consider a few terms in Eq. (3.1). Now we can move on to the second factor, i.e. N^*. To find the total number of terms necessary for a desired accuracy, we recall that Eq. (3.1) has the structure of Zernike polynomials; i.e. $n \geq m, \quad n, m > 0, \quad$ and $n - m =$even. Using elementary number theory, one can conclude that the total number of necessary terms in Eq. (3.1) is

$$N^* = \left\lfloor \frac{n^*+2}{2} \right\rfloor \left\lceil \frac{n^*+2}{2} \right\rceil . \tag{4.5}$$

Apparently, the number of terms in A_{nm} depends on $\aleph_m$ and $S^m_{n,k_N}(\beta)$, which both in turn depend on the value of N_j^*s. This is due to the Taylor expansion that we have used. Using the analysis in Appendix B and the values of N_j^*, we can determine the complexity of the A_{nm}. The coefficients A_{nm} are polynomials of the aberration constants of order no more than N_j^* for each particular aberration coefficient. The A_{nm}s also depend on the defocus coefficient both in the form of rational polynomial of order no more than $1 + (n+m)/2 + \sum_{j\in\chi_4} N_j{}^*$ and in the form of $\exp(\beta_1)$, where χ_4 is in Eq. (4.6) . Hence, it is clear that increasing defocus does not increase the complexity of coefficients A_{nm} in a confined region of interest.

$$\chi_4 = \{j | \, L_j \neq 0,\, j = 2, \ldots, n_{ab}\} \tag{4.6}$$

4.3 Numerical v.s. Theoretical Results

Although the above analysis gives us a comprehensive understanding of an upper bound on the complexity of calculating the light disturbance within the exit window R^*, the bounds presented might be loose as suggested by numerical experiment. For instance, for the case of $R^* = 40$ and $\epsilon = 0.001$, using Theorem 4.2.1, $n^* = 81$;

whereas experimental result suggests $n^* = 45$. Nevertheless, Theorem 4.2.1 is the tightest theoretical bound currently available.

Performing the same experiment for different values of R^* suggests that $n^* = \lceil R^* \rceil + 5$ suffices for $\epsilon = 0.001$. Replacing n^* in Eq. (4.5) by its experimental value , i.e. $\lceil R^* \rceil + 5$, one can get the following expression for the total number of necessary terms in Eq. (3.1) (or Eq. (4.1)) for an accuracy of $\epsilon = 0.001$ in a desired range R^*

$$N^* = \left\lfloor \frac{\lceil R^* \rceil + 7}{2} \right\rfloor \left\lceil \frac{\lceil R^* \rceil + 7}{2} \right\rceil . \tag{4.7}$$

The above two equations show the necessary number of terms to express the diffraction integral within a desired range and accuracy. This is of much greater importance when we recall that the number of terms required in the expansion is independent of the values of aberrations and defocus and the required resolution. In other words, regardless of the properties of the imaging system, the above number of terms is sufficient for calculating the light disturbance in the image plane. For instance for an optical system with $f = 50mm$, $f/\# = 3mm$ and pixel-size= $5\mu m$, if we consider a circle with radius of 5 pixels around each pixel and accuracy of $\epsilon = 0.001$, then R^* is 47.5 and thus we do not need to consider terms with $n > 53$ no matter how large our defocus or aberrations are or how fine our resolution is.

We have also performed experiments for finding the minimum number of Taylor expansion terms necessary for each aberration, N_j^*, for an accuracy of $\epsilon = 0.001$ and range of interest of $R^* = 20$. These results are shown in Fig. 4-1. One can notice

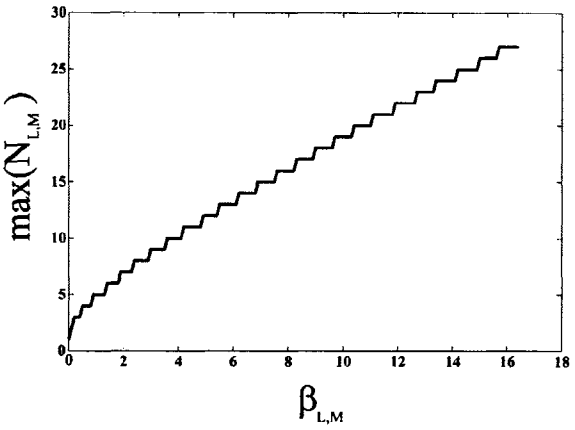

Figure 4-1: Variation of partial number of the terms necessary with $\beta_{L,M}$ for $\epsilon = 0.001$ and $R^* = 20$.

the gap between the theoretical and experimental bounds by comparing Theorem 4.2.1 and Fig. 4-1. For instance for $|\beta| = 5$, using Theorem 4.2.1 one gets $N_j^* = 29$, whereas experimental results suggest $N_j^* = 11$.

Note that without considering the number of aberrations present and their range of values, we cannot state a general result about the absolute or relative errors of this approximation (Eq. (3.1)) in the whole infinite image plane; i.e when $R^* \rightarrow \infty$. For instance, when the distortion aberration coefficient (γ_3) is large, the PSF peak can shift out of the exit window, causing the absolute and relative approximation errors to increase without bound. This example is shown in Fig. 4-2.

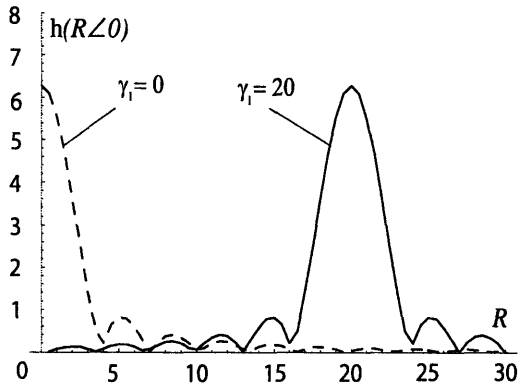

Figure 4-2: Radial variation of modulus of the PSF with and without Distortion (normalized to 2π).

Chapter 5

Discussions

5.1 Overview

Eqs. (3.1) and (3.4) are general expressions for the study of the effect of aberrations and defocus on PSF on the basis of diffraction theory. Two important points that are hidden in these equations are their ability to handle high defocus cases without facing any numerical problems and the potential of this method to consider the effect of as many aberrations as needed at the same time as defocus. In fact any arbitrary aberration can be approximated using Eq. (2.7) and then its effect on the imaging system will be immediately available.

This latter property is very useful in Wavefront Coding (WFC). [6, 11] In this technique we use general aberrated optical elements (traditionally aspheric) and digital post processing together to increase the performance and/or decrease the cost of imaging systems. In another work [1] which is under preparation, the advantages of using this new approach for solving the diffraction integral in WFC are investigated.

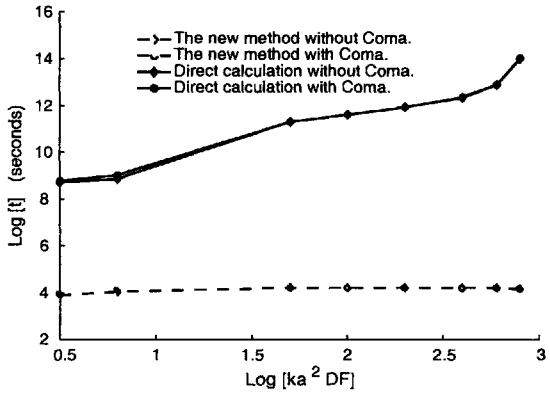

Figure 5-1: Time required for evaluating the PSF at 400 different points v.s. defocus ($\epsilon = 0.1\%$).

5.2 Convergence Speed

Another important fact about this method is its fast performance compared to direct calculation. It is often the case that direct ray tracing does not suffice for practical needs and one has to analyze the effect of aberrations and defocus using diffraction theory. In that case, our method proves to be very efficient. Figure 5-1 shows the time required to evaluate the PSF at 400 different points in the image plane. It can be seen that for all values of aberrations and defocus, the time required by the new method is significantly smaller. The ratio of time needed varies from 150 for zero defocus to more than 2000 for defocus of 785 wave numbers (or 125 waves or $125\lambda\, mm$ or $\beta_1 = 785\,\mathbf{i}$). It should be noted that in all of the calculations in this figure, the accuracy has been kept at 0.1%.

It is to be noted that the traditional method mentioned in Fig. 5-1 is the direct evaluation of the diffraction integral. It is a common practice to use fast Fourier transform (FFT) rather than direct integration, to enhance the speed of calculation. Although FFT method is almost invariant to defocus and aberration coefficient values,

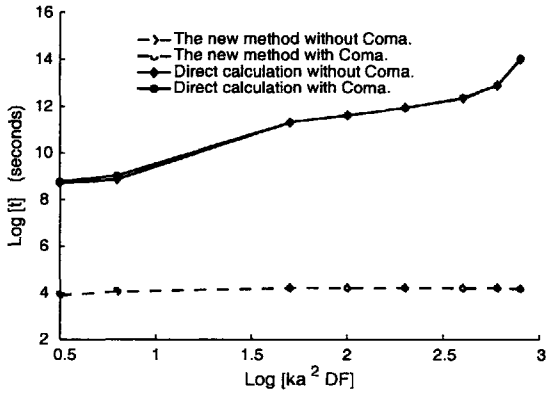

Figure 5-1: Time required for evaluating the PSF at 400 different points v.s. defocus ($\epsilon = 0.1\%$).

5.2 Convergence Speed

Another important fact about this method is its fast performance compared to direct calculation. It is often the case that direct ray tracing does not suffice for practical needs and one has to analyze the effect of aberrations and defocus using diffraction theory. In that case, our method proves to be very efficient. Figure 5-1 shows the time required to evaluate the PSF at 400 different points in the image plane. It can be seen that for all values of aberrations and defocus, the time required by the new method is significantly smaller. The ratio of time needed varies from 150 for zero defocus to more than 2000 for defocus of 785 wave numbers (or 125 waves or $125\lambda\, mm$ or $\beta_1 = 785\,\mathrm{i}$). It should be noted that in all of the calculations in this figure, the accuracy has been kept at 0.1%.

It is to be noted that the traditional method mentioned in Fig. 5-1 is the direct evaluation of the diffraction integral. It is a common practice to use fast Fourier transform (FFT) rather than direct integration, to enhance the speed of calculation. Although FFT method is almost invariant to defocus and aberration coefficient values,

(3.1) and maximum necessary degree of polynomials for Eq. (3.4) which together provide us with an accurate approximation within the region of interest. This theorem also supplies an upper bound for the maximum necessary index of summation and maximum necessary degree of polynomials. Nevertheless numerical experiments suggest that even smaller bounds would suffice. Equation (4.7) provides us with one such experimental result. It shows the total number of terms necessary in Eq. (3.1) for an accuracy of $\epsilon = 0.001$.

5.3 Other Advantages

Another interesting property of our expansion is its advantage in facilitating the process of calculating the amplitude transfer function (ATF), optical transfer function (OTF), and modulation transfer function(MTF) for an imaging system. This is due to elegant choice of basis functions; for instance, to move from the the PSF domain to OTF domain, one needs to change the basis functions only. In other words, this process does not demand any extra calculation and the coefficients that have been calculated for point spread function domain, can be used directly for other domains too. This subject will be thoroughly discussed in another work which is under preparation.

Chapter 6

Conclusions

In this thesis we introduced a new method for analyzing the diffraction integral and evaluating the PSF. The new method is based on the use of higher order Airy functions along with a novel use of Zernike and Taylor expansions. This method is applicable when we are considering several aberrations and large defocus simultaneously. We have shown rigorously and verified by numerical simulations that the complexity of our expansion is independent of defocus and that it is stable in all ranges of defocus. The efficiency of the method compared to traditional ones has also been investigated and it is shown that the method not only does extremely faster than its alternates but also requires computational time that is independent of defocus.

The use of higher order Airy functions plays a key role in capturing the effect of different values of defocus in a simple expression which its complexity is independent of defocus. It was also shown in Theorem 4.2.1, that any arbitrary accuracy in any arbitrary region of interest could be achieved by a finite number of terms in the approximate function (Eq. (4.1)).

The complexity of this expansion is also invariant to resolution. This means that the time required for evaluating the PSF will not increase as the desired resolution increases. This could be a potential solution to some of the current problems in biological microscopy [8] and lithography [13] where having a high resolution information of PSF is critical. By providing an analytical solution for the diffraction integral, this approach, among other things, may also facilitate the process of multi-domain optimization, where the optical system and post-processing system are optimized together to increase the performance and/or reduce the cost of imaging systems. This analytical expression for PSF may also help developing analytic treatment of incoherent imaging systems.

Appendix A

Table of Symbols

Term	Symbol	Definition
Point spread function (PSF)	h	Eqs. (2.2)
Normalized PSF	$\hat{h}$	Eqs. (2.12) (3.1)
Approximated normalized PSF	$\hat{h}_{n^*}$	Eqs. (4.1)
Coefficient of the diffraction integral	C	Eq. (2.9)
First index of expansion	n	-
Second index of expansion	m	-
Coord. system in image plane	(x, y)	Fig. 2-1
Polar coord. system in image plane	$r\angle\phi$	Fig. 2-1

continued on next page

continued from previous page

Term	Symbol	Definition
Coord. system in object plane	(x_0, y_0)	Fig. 2-1
Polar coord. system in object plane	$r_0 \angle \phi_0$	Fig. 2-1
Axillary coord. system	(u, v)	Eqs. (2.3) (2.4)
Polar axillary coord. system	$R \angle \Theta$	Pol. equiv. of (u, v)
Coord. system in pupil plane	(ξ, η)	Fig. 2-1
Polar coord. system in pupil plane	$\rho \angle \theta$	Pol. equiv. of (ξ, η)
Simplified coefficient of expansion	A'_{nm}	-
Main coefficient of expansion	A_{nm}	Eq. (3.4)
Approximated main coefficient of expansion	A^*_{nm}	Eq. (4.2)
Matrix of image	$\vec{Q}$	-
Matrix of object	$\vec{P}$	-
One point at image plane	$Q(x, y)$	Fig. 2-1
One point at object plane	$P(x_0, y_0)$	Fig. 2-1
Area of interest in object plane	$\mathcal{A}$	-
Wave number	k	$2\pi/\lambda$
Circular aperture radius	a	Fig. 2-1
Distance from each image point to the		

continued on next page

continued from previous page

Term	Symbol	Definition
center of pupil plane	$s^{'}$	Eq. (2.6)
Distance from each object point to the center of pupil plane	$r^{'}$	Eq. (2.5)
Distance between image plane and pupil plane	S_Q	Fig. 2-1
Distance between object plane and pupil plane	S_P	Fig. 2-1
Distance between Gaussian image plane and pupil plane	S_G	-
Wavefront error	w	Eq. (2.7)
Defocus coefficient	DF	Eq. (2.8)
Index of different aberrations	L, M	Eq. (2.7)
Aberration coefficient	$f_{L,M}$	Eq. (2.7)
Final aberration coefficient	β_j	Eq. (3.7)
Aberration Taylor expansion index	N_j	Eqs. (3.6) (4.3)
Vector of different aberration's Taylor expansion indices	$\mathbf{N}$	Eqs. (3.6) (4.3)

continued on next page

continued from previous page

Term	Symbol	Definition
Value of an integration	D	Eqs. (3.6) (4.3)
Set containing all feasible pairs of **N** and D	$\aleph_m$	Eq. (3.6)
Approximated set containing all feasible pairs of **N** and D	$\aleph_m^*$	Eq. (4.3)
Vector containing all final aberration coefficients	$\vec{\beta}$	-
Multiply of final aberration coefficients according to the values of **N**	$\beta_{\mathbf{N}}$	Eq. (3.8)
Power of ρ	$k_{\mathbf{N}}$	Eq. (3.9)
S function	$S^m_{n,k_{\mathbf{N}}}$	Eq. (3.6)
Approximated S function	${S^m_{n,k_{\mathbf{N}}}}^*$	Eq. (4.4)
Polynomial part of the Zernike function	R^m_n	Eq. (B.2)
Zernike function	V^m_n	Eq. (B.1)
Index of coefficients of Zernike polynomial	l	Eq. (B.3)
Zernike polynomial coefficients	$C^m_{n,l}$	Eq. (B.3)
Defocus and Field Curvature aberration		

continued on next page

continued from previous page

Term	Symbol	Definition
final Coefficient	γ_1	Eq. (3.13)
Spherical aberration final coefficient	γ_2	Eq. (3.13)
Distortion aberration final coefficient	γ_3	Eq. (3.13)
Astigmatism aberration final coefficient	γ_4	Eq. (3.13)
Coma aberration final coefficient	γ_5	Eq. (3.13)
Distortion Taylor expansion index	N_3	-
Astigmatism Taylor expansion index	N_4	-
Coma Taylor expansion index	N_5	-
Scaling factor between R and r	B	ka/s'
focal length	f	-
focal number	$f/\#$	$f/2a$
The critical radius of interest	R^*	Theorem 4.2.1
The minimum necessary index of summation in Eq. (4.1) necessary for a given accuracy	n^*	Theorem 4.2.1
The minimum necessary number of terms in the Taylor expansion for each aberration necessary for a given accuracy	N_j^*	Theorem 4.2.1

continued on next page

continued from previous page

Term	**Symbol**	**Definition**
The minimum total number of terms in Eq. (4.1) necessary for a given accuracy	N	Eq. (4.5)

Appendix B

Derivation of the Expansion for the Point Spread Function

We now derive expressions in Eqs. (3.1) and (3.4) for the PSF. Rather than following the traditional approach of expanding the wavefront phase, w, using Zernike polynomials [2], in the first step of analyzing Eq. (2.12), we expand the exponential of the wavefront phase, $\exp(\mathbf{i}\,kw)$, using the set of Zernike polynomials, $V_n^m(\rho,\theta)$

$$V_n^m(\rho,\theta) = R_n^{|m|}(\rho)\mathrm{e}^{\mathbf{i}\,m\theta}. \tag{B.1}$$

Here $n \geq 0$ and m are integers, $n \geq |m|$ and $n-|m|$ is even. Furthermore $R_n^{|m|}(\rho)$ is defined as

$$R_n^{|m|}(\rho) = \sum_{l=0}^{(n-|m|)/2} C_{n,l}^m \rho^{n-2l}, \tag{B.2}$$

where

$$C_{n,l}^{m} = \frac{(-1)^l (n-l)!}{l![(n+m)/2-l]![(n-m)/2-l]!}. \tag{B.3}$$

Thus we can rewrite the wavefront $e^{i\,k\,w(\rho,\theta,r_0,\phi_0)}$ as

$$e^{i\,k\,w(\rho,\theta,r_0,\phi_0)} = \sum_{n=0}^{\infty} \sum_{|m|=0}^{n} \left[\tilde{\delta}_{n-m} A_{nm} R_n^{|m|}(\rho) e^{i\,m\theta} \right], \tag{B.4}$$

where $\tilde{\delta}_i$ is equal to 1 if i is even and 0 otherwise. A_{nm} in Eq. (B.4) is defined as

$$A_{nm} = \frac{n+1}{\pi} \int_0^1 \int_0^{2\pi} e^{i\,k\,w(\rho,\theta,r_0,\phi_0)}\, V_n^m(\rho,\theta)\, \rho\, d\rho\, d\theta. \tag{B.5}$$

Recalling the definition of $\hat{h}$ in Eq. (2.12) and using (B.4), we have

$$\begin{aligned} \hat{h}(x,y;x_0,y_0) \;=\; & \frac{1}{2\pi} \int_0^1 \int_0^{2\pi} \left\{ \sum_{n=0}^{\infty} \sum_{|m|=0}^{n} \left[\tilde{\delta}_{n-m} A_{nm} R_n^{|m|}(\rho) e^{i\,m\theta} \right] \right\} \\ & e^{iR\rho\cos(\theta-\Theta)} \rho\, d\rho\, d\theta. \end{aligned} \tag{B.6}$$

Using the definition of Bessel function [12], we have

$$\int_0^{2\pi} e^{i\,m\theta} e^{iR\rho\cos(\theta-\Theta)} d\theta = 2\pi e^{i\,m\Theta}\, i^{\,m} J_m(R\rho),$$

therefore we can rewrite Eq. (B.6) as

$$\hat{h}(x,y;x_0,y_0) \;=\; \int_0^1 \left\{ \sum_{n=0}^{\infty} \sum_{|m|=0}^{n} \left[\tilde{\delta}_{n-m} A_{nm} R_n^{|m|}(\rho) e^{i\,m\Theta}\, i^{\,m} J_m(R\rho) \right] \right\} \rho\, d\rho. \tag{B.7}$$

Now applying the following property of Zernike polynomials [2]

$$\int_0^1 R_n^{|m|}(\rho)\, J_m(R\rho)\, \rho\, d\rho = (-1)^{\frac{n-m}{2}}\, \frac{J_{n+1}(R)}{R}, \tag{B.8}$$

we can evaluate the integral in Eq. (B.7) as

$$\hat{h}(x, y; x_0, y_0) \;=\; \sum_{n=0}^{\infty} \sum_{|m|=0}^{n} \left[\tilde{\delta}_{n-m} A_{nm} \mathrm{e}^{\mathrm{i}\, m\Theta}\, \mathrm{i}^{\,m} (-1)^{\frac{n-m}{2}}\, \frac{J_{n+1}(R)}{R} \right]. \tag{B.9}$$

Now we are concerned with evaluating the Zernike coefficient. This is equivalent to evaluating the integral in Eq. (B.5). Although at first sight it appears that solving Eq. (B.5) and Eq. (2.12) are both equally hard, as it will become clear Eq. (B.5) has several advantages over Eq. (2.12). The most important advantage is that we can evaluate the integral analytically in this new expression without expanding the defocus term (This is addressed in more detail in Appendix C). This allows us to have the result of arbitrarily large defocused system readily available. Another important property of this method is its fast convergence which is discussed in chapter 4 and Appendix D. To solve Eq. (B.5), we first partially expand $\mathrm{e}^{\mathrm{i}\, k\, w(\rho,\theta,r_0,\phi_0)}$ using Taylor series as follows:

$$
\begin{aligned}
e^{\mathbf{i}\,k\,w(\rho,\theta,r_0,\phi_0)} &= e^{\mathbf{i}\,k\,\sum_{j=1}^{n_{ab}}\left[f_{L_j\cdot M_j}(r_0{}^2)\,(a\,\rho)^{2L_j}\,(a\,\rho\,\cos(\theta-\phi_0))^{M_j}\right]} \\
&= e^{\sum_{j=1}^{n_{ab}}\left[\beta_j\,\rho^{2L_j+M_j}\,\cos^{M_j}(\theta-\phi_0)\right]} \\
&= e^{\sum_{j\in\chi_1}\left[\beta_j\,\rho^{2L_j}\right]}\,e^{\sum_{j\in\chi_2}\left[\beta_j\,\rho^{2L_j+M_j}\,\cos^{M_j}(\theta-\phi_0)\right]} \\
&= e^{\sum_{j\in\chi_1}\left[\beta_j\,\rho^{2L_j}\right]}\prod_{j\in\chi_2} e^{\beta_j\,\rho^{2L_j+M_j}\,\cos^{M_j}(\theta-\phi_0)} \\
&= e^{\sum_{j\in\chi_1}\left[\beta_j\,\rho^{2L_j}\right]}\times \\
&\quad \prod_{j\in\chi_2}\left\{\sum_{N_j=0}^{\infty}\frac{\left[\beta_j\,\rho^{2L_j+M_j}\,\cos^{M_j}(\theta-\phi_0)\right]^{N_j}}{N_j!}\right\},
\end{aligned}
\tag{B.10}
$$

where N_j is the summation variable for each of terms in aberration function which have been Taylor expanded and β_j is defined as

$$
\beta_j = \mathbf{i}\,k\,f_{L_j,M_j}(r_0{}^2)\,a^{2L_j+M_j}. \tag{B.11}
$$

Substituting Eq. (B.10) in Eq. (B.5), we have

$$
\begin{aligned}
A_{nm} &= \frac{n+1}{\pi}\int_0^1\int_0^{2\pi} e^{\sum_{j\in\chi_1}\left[\beta_j\,\rho^{2L_j}\right]}\times \\
&\quad \prod_{j\in\chi_2}\left\{\sum_{N_j=0}^{\infty}\frac{\left[\beta_j\,\rho^{2L_j+M_j}\,\cos^{M_j}(\theta-\phi_0)\right]^{N_j}}{N_j!}\right\}\times \\
&\quad V_n^m(\rho,\theta)\,\rho\,d\rho\,d\theta.
\end{aligned}
\tag{B.12}
$$

Integrating over θ yields

$$A_{nm} = \frac{n+1}{2^{m-1}} \mathrm{e}^{\mathrm{i}\, m\phi_0} \int_0^1 \mathrm{e}^{\sum_{j\in\chi_1}\left[\beta_j \rho^{2L_j}\right]} R_n^{|m|}(\rho) \left\{ \sum_{(\mathbf{N},D)\in\aleph_m} D \prod_{j\in\chi_2} \frac{\left[\beta_j \rho^{2L_j+M_j}\right]^{N_j}}{N_j!} \right\} \rho\, d\rho, \tag{B.13}$$

where we have used the orthogonality property of trigonometry functions

$$\begin{aligned}
\forall\, m, m' \quad &: \int_0^{2\pi} \sin(m\theta)\,(\cos(\theta))^{m'}\, d\theta = 0. \\
\forall\, m > m' \quad &: \int_0^{2\pi} \cos(m\theta)\,(\cos(\theta))^{m'}\, d\theta = 0, \\
\forall\, m < m' = m+2k+1 \quad &: \int_0^{2\pi} \cos(m\theta)\,(\cos(\theta))^{m+2k+1}\, d\theta = 0, \\
\forall\, m < m' = m+2k \quad &: \int_0^{2\pi} \cos(m\theta)\,(\cos(\theta))^{m+2k}\, d\theta = \frac{\pi(m+2k)!}{2^{2k+m-1}k!(m+k)!},
\end{aligned} \tag{B.14}$$

where m, m' $(m \neq m')$ and k are positive integers. Note that this leaves us with only a few sets of cross terms to deal with as stated in Eq. (B.13) (rather than an infinite number of terms of the Taylor expansion of the aberrations for the term A_{nm}). $\mathbf{N} = [N_2, N_3, \ldots N_{n_{ab}}]$ in Eq. (B.13) is a vector containing the values for all N_js. Furthermore, $\aleph_m$, which is a set containing all pairs of vectors in the form $\mathbf{N}$ and scalars D, is defined as

$$\aleph_m = \left\{ (\mathbf{N}, D) \;|\; \sum_{j=2}^{n_{ab}} (M_j N_j) = |m| + 2k,\; D = \frac{(m+2k)!}{2^{2k}k!(m+k)!};\; k, N_j \in \mathcal{N} \right\}. \tag{B.15}$$

Also using the special dependence of Eq. (B.13) on m and by defining δ_i as one when $m = 0$ and as two otherwise, we can further simplify Eqs. (B.9) and (B.13) as

$$\hat{h}(x, y; x_0, y_0) = \sum_{n=0}^{\infty} \sum_{m=0}^{n} \left\{ \tilde{\delta}_{n-m} \delta_m A_{nm} \cos\left[m(\Theta + \phi_0)\right] \frac{J_{n+1}(R)}{R} \right\}, \quad \text{(B.16)}$$

$$A_{nm} = \frac{n+1}{2^{m-1}} \mathbf{i}^n \sum_{(\mathbf{N}, D) \in \Re_m} D\, \beta_{\mathbf{N}}\, S^m_{n,k_{\mathbf{N}}}(\vec{\beta}), \quad \text{(B.17)}$$

and consider m to be a positive integer. Note that $\beta_{\mathbf{N}}$ and $S^m_{n,k_{\mathbf{N}}}(\vec{\beta})$ are defined as

$$S^m_{n,k_{\mathbf{N}}}(\vec{\beta}) = \int_0^1 \prod_{j \in \chi_1} \mathrm{e}^{\beta_j \rho^{2L_j}}\, R^m_n(\rho)\, \rho^{k_{\mathbf{N}}+1}\, d\rho, \quad \text{(B.18)}$$

$$\beta_{\mathbf{N}} = \prod_{j \in \chi_2} \frac{(\beta_j)^{N_j}}{N_j!}. \quad \text{(B.19)}$$

And we have

$$k_{\mathbf{N}} = \sum_{j \in \chi_2} (2L_j + M_j) N_j. \quad \text{(B.20)}$$

Appendix C

Derivation of the $S^m_{n,k_{\mathbf{N}}}(\vec{\beta})$ in Equation (3.6)

Using Eqs. (3.6) and (B.2) and considering the fact that $m > 0$, we have

$$S^m_{n,k_{\mathbf{N}}}(\vec{\beta}) = \int_0^1 \prod_{j\in\chi_1} \mathrm{e}^{\beta_j \rho^{2L_j}} \sum_{l=0}^{(n-m)/2} C^m_{n,l}\rho^{n-2l+k_{\mathbf{N}}+1}\, d\rho. \tag{C.1}$$

Assuming that the summations involved are finite (which means that the number of aberrations under consideration is finite), we have

$$S^m_{n,k_{\mathbf{N}}}(\vec{\beta}) = \sum_{l=0}^{(n-m)/2} C^m_{n,l} \int_0^1 \prod_{j\in\chi_1} \mathrm{e}^{\beta_j \rho^{2L_j}} \rho^{n-2l+k_{\mathbf{N}}+1}\, d\rho. \tag{C.2}$$

Using Eqs. (B.14) and (B.20) we can see that $k_{\mathbf{N}} \geq 0$ and $k_{\mathbf{N}} = m + 2\acute{k}$. On the other hand from the definition of the Zernike polynomials we know that $n+m$ is also an even number. Thus it follows that $n - 2l + k_{\mathbf{N}}$ is an even number. This is an important property of our expansion and a key factor in the derivation that follows.

The next step is to replace each term of $e^{\beta_j \rho^{2L_j}}$ in Eq. (C.2) by its Taylor expansion

$$S^m_{n,k_{\mathbf{N}}}(\vec{\beta}) = \sum_{l=0}^{(n-m)/2} C^m_{n,l} \int_0^1 e^{\beta_1 \rho^2} \prod_{j \in \chi_3} \left[\sum_{N_j=0}^{\infty} \frac{(\beta_j \rho^{2L_j})^{N_j}}{N_j!} \right] \rho^{n-2l+k_{\mathbf{N}}+1} \, d\rho. \tag{C.3}$$

Thus the solution of the above general form requires the solution of the integral

$$\int_0^1 e^{\beta_1 \rho^2} \rho^{2\tau+1} \, d\rho, \tag{C.4}$$

where $\tau = \frac{n+k_{\mathbf{N}}}{2} + l + \sum_{j \in \chi_3} L_j N_j$ is an integer number. Note that since $N_j \in \mathcal{N}$, there will be infinite number of fundamental integral to solve. However to remain in the range of desired accuracy, we only need to use $N_j \in \{0, \ldots, N_j^*\}$, where N_j^* depends on the problem specification and the respective accuracy. Theorem 4.2.1 provides us with an upper bound for N_j^* for a prescribed desired accuracy and problem specifications.

To solve the fundamental integral in Eq. (C.4), we can use the technique of integration by parts τ times to get

$$\frac{(-\beta_1)^{-(\tau+1)}}{2} \tau! \left[1 - e^{\beta_1} \sum_{k=0}^{\tau} \frac{(-\beta_1)^k}{k!} \right]. \tag{C.5}$$

Using this result, one can find the general formula for S. For instance when $\beta_{L,0} = 0$ for $L \geq 2$, we have

$$S^m_{n,k_{\mathbf{N}}}(\vec{\beta}) = \sum_{l=0}^{(n-m)/2} \left(\frac{C^m_{n,l}}{2} (-\beta_1)^{\frac{-(2+n-2l+k_{\mathbf{N}})}{2}} (\frac{n-2l+k_{\mathbf{N}}}{2})! \left[1 - \mathrm{e}^{\beta_1} \sum_{j=0}^{\frac{n-2l+k_{\mathbf{N}}}{2}} \frac{(-\beta_1)^j}{j!} \right] \right). \quad \text{(C.6)}$$

Here $S^m_{n,k_{\mathbf{N}}}(\vec{\beta})$ is a rational polynomial of order $1+(n+k)/2$ of β_1. There is also one $\exp(\beta_1)$ factor in the structure of $S^m_{n,k_{\mathbf{N}}}(\vec{\beta})$. Thus we can conclude that in case of primary aberrations $S^m_{n,k_{\mathbf{N}}}(\vec{\beta})$ is a rational polynomial of order $1+(n+m)/2+{N_{S.A.}}^*+{N_{Coma}}^*$ of β_1. In general the order of this polynomial is $1+(n+m)/2+\sum_{j\in\chi_4}{N_j}^*$.

For any given accuracy, there is a value of $|\beta_1|$ for which, it may be more efficient to use the method of stationary phase. For instance when $\epsilon = 0.001$, for $|\beta_1| > 700$, it may be more efficient to use the method of stationary phase. In what follows we consider such a case. Note that in practice this is equivalent to the case that the defocus is large enough that the PSF will become almost constant.

Using the fact that $k_N = m + 2\acute{k}$, by changing the variable of ρ^2 to ρ and β_1 to $\mathbf{i}\,\acute{\beta}$ ($\acute{\beta} \in \Re$), we can rewrite Eq. (C.1) as

$$
\begin{aligned}
S^m_{n,k_{\mathbf{N}}}(\beta_1) &= \sum_{l=0}^{(n-m)/2} C^m_{n,l} \int_0^1 \mathrm{e}^{\mathbf{i}\acute{\beta}\rho} \rho^{\frac{n+m}{2}-l+\acute{k}}\, d\rho \qquad \text{(C.7)} \\
&\approx \sum_{l=0}^{(n-m)/2} C^m_{n,l} \int_0^1 \left[\cos(\acute{\beta}\rho) + \mathbf{i}\ \rho\ \sin(\acute{\beta}\rho)\right] d\rho \\
&= \sum_{l=0}^{(n-m)/2} C^m_{n,l} \frac{\mathrm{e}^{\mathbf{i}\acute{\beta}}}{\mathbf{i}\acute{\beta}} \\
&= \frac{\mathrm{e}^{\mathbf{i}\acute{\beta}}}{\mathbf{i}\acute{\beta}} \sum_{l=0}^{(n-m)/2} C^m_{n,l} \\
&= \frac{\mathrm{e}^{\mathbf{i}\acute{\beta}}}{\mathbf{i}\acute{\beta}} \\
&= \frac{\mathrm{e}^{\beta_1}}{\beta_1}.
\end{aligned}
$$

In the above derivation, we have assumed that $k_{\mathbf{N}} > 0$; if this is not the case, i.e. $k_{\mathbf{N}} = 0$, then using the same method one can show that

$$
S^m_{n,k_{\mathbf{N}}}(\beta_1) = \frac{\mathrm{e}^{\beta_1} + (-1)^{\frac{n+1}{2}}}{\beta_1}. \qquad \text{(C.8)}
$$

Appendix D

Complexity Proofs

Lemma D1. *For all A_{nm} defined by Eq. (3.4), we have the following bound*

$$|A_{nm}| \leq \sqrt{n+1}. \tag{D1}$$

Proof: Using Eq. (3.4) we have

$$A_{nm} = \frac{n+1}{\pi} \int_0^1 \int_0^{2\pi} \mathrm{e}^{\mathbf{i}\, k w(\rho,\theta,r_0,\phi_0)}\, \mathrm{e}^{\mathbf{i}\, m\theta}\, R_n^m(\rho)\, \rho\, d\rho\, d\theta, \tag{D2}$$

thus

$$|A_{nm}| \leq 2(n+1) \int_0^1 |R_n^m(\rho)|\, \rho\, d\rho. \tag{D3}$$

Using the Cauchy-Schwarz inequality, we have

$$\int_a^b \Psi(u)\, du \leq \sqrt{\int_a^b \Psi^2(u)\, du}, \tag{D4}$$

for any real valued integrable function Ψ, and real numbers a and b. Now considering the fact that in Eq. (D3), $\rho \in [0,1]$ and thus $\rho \geq 0$, we can define $\sqrt{u} = \rho$. Replacing Ψ with $|R_n^m(\rho)|$ and setting $a = 0$ and $b = 1$ in Eq. (D4) yields

$$\begin{aligned} \int_0^1 |R_n^m(\rho)|\, \rho\, d\rho &= \frac{1}{2}\int_0^1 |R_n^m(\sqrt{u})|\, du \\ &\leq \frac{1}{2}\sqrt{\int_0^1 \left[R_n^m(\sqrt{u})\right]^2 du} \\ &= \sqrt{\frac{1}{2}\int_0^1 \left[R_n^m(\rho)\right]^2 \rho\, d\rho}, \end{aligned} \tag{D5}$$

where the right-hand-side integral is readily available from orthogonality analysis of the Zernike polynomials [2]

$$\int_0^1 \left[R_n^m(\rho)\right]^2 \rho\, d\rho = \frac{1}{2(n+1)}. \tag{D6}$$

Hence, we have

$$\int_0^1 |R_n^m(\rho)|\, \rho\, d\rho \leq \frac{1}{2\sqrt{n+1}}. \tag{D7}$$

Substituting this result in Eq. (D3), we have

$$|A_{nm}| \leq \sqrt{n+1} \tag{D8}$$

□

Let $T_n^f(x)$ be the n^{th} term in the Taylor expansion of $f(x)$ around $x_0 = 0$, then we have the following Lemma about the accuracy of the Taylor expansion.

Lemma D2. *Let*

$$f(x) = \mathrm{e}^{bx^m},$$

where b is an imaginary number and $x \in [0,1]$. If

$$p^* = \max\left(4,\ 2\mathrm{e}\,|b| + 1,\ \log_2 \frac{\mathrm{e}}{(2\mathrm{e}-1)\sqrt{2\pi}\epsilon}\right).$$

Then we have

$$\left| f(x) - \sum_{n=0}^{mp^*} T_n^f(x) \right| \leq \epsilon\,|f(x)|\,.$$

Proof: Using Taylor Theorem we have

$$\begin{aligned} \left| f(x) - \sum_{n=0}^{mp^*} T_n^f(x) \right| &= \left| \sum_{n=mp^*+1}^{\infty} T_n^f(x) \right| \\ &= \left| \sum_{n=mp^*+1}^{\infty} \frac{f^n(0)}{n!} x^n \right|. \end{aligned} \tag{D9}$$

Using the definition of f, we have

$$f^n(0) = \begin{cases} 0 & \text{if } n \neq mp\ , \\ n!\frac{b^p}{p!} & \text{if } n = mp. \end{cases} \tag{D10}$$

where p is a positive integer. Substituting this in Eq. (D9) and changing the index of summation from n to p, we have

$$\begin{aligned} \left| f(x) - \sum_{n=0}^{mp^*} T_n^f(x) \right| &= \left| \sum_{p=p^*}^{\infty} \frac{b^p}{p!} x^{mp} \right| \\ &\leq \left| \sum_{p=p^*}^{\infty} \frac{b^p}{p!} \right| \\ &\leq \sum_{p=p^*}^{\infty} \frac{|b|^p}{p!} \\ &\leq \sum_{p=p^*}^{\infty} \frac{|b|^p}{p^*!\, p^{*p-p^*}} \\ &= \frac{|b|^{p^*}}{p^*!} \sum_{p=p^*}^{\infty} \left(\frac{|b|}{p^*} \right)^p \\ &\leq \frac{|b|^{p^*}}{p^*!} \sum_{p=p^*}^{\infty} \left(\frac{1}{2\mathrm{e}} \right)^p \\ &= \frac{|b|^{p^*}}{p^*!} \frac{2\mathrm{e}}{2\mathrm{e}-1} \end{aligned} \tag{D11}$$

The first inequality follows from $x \in [0, 1]$. The third inequality follows from $p! \geq p^*! p^{*p-p^*}$. The fourth inequality follows from $p^* \geq 2\mathrm{e}\,|b| + 1$. We can further simplify this expression as in Eq. (D12).

$$\begin{aligned}
\left| f(x) - \sum_{n=0}^{mp^*} T_n^f(x) \right| &= \frac{|b|^{p^*}}{p^*!} \frac{2\mathrm{e}}{2\mathrm{e}-1} \qquad \text{(D12)} \\
&\leq \frac{|b|^{p^*}}{\sqrt{2\pi} p^{*p^*+0.5} \mathrm{e}^{-p^*}} \frac{2\mathrm{e}}{2\mathrm{e}-1} \\
&= \left(\frac{|b|\,\mathrm{e}}{p^*} \right)^{p^*} \frac{2\mathrm{e}}{(2\mathrm{e}-1)\sqrt{2\pi p^*}} \\
&\leq \left(\frac{1}{2} \right)^{p^*} \frac{2\mathrm{e}}{(2\mathrm{e}-1)\sqrt{2\pi p^*}} \\
&\leq \left(\frac{1}{2} \right)^{p^*} \frac{\mathrm{e}}{(2\mathrm{e}-1)\sqrt{2\pi}} \\
&\leq \epsilon \\
&\leq |f(x)|\,\epsilon.
\end{aligned}$$

In the first inequality, we have applied the following lower bound to $p^*!$, based on Stirling's approximation:

$$\sqrt{2\pi} p^{*p^*+0.5} \exp(-p^*) \leq p^*!.$$

The second inequality follows from $p^* \geq 2e\,|b| + 1$. The third inequality follows from $p^* \geq 4$. In the fourth inequality we have used $p^* \geq \log_2 \frac{\mathrm{e}}{(2\mathrm{e}-1)\sqrt{2\pi\epsilon}}$. In the fifth inequality we have used $|\exp(\mathbf{i}\,x)| = 1$ for all $x \in \Re$.

□

Lemma D3. *For all $R \in \Re$ we have*

$$\sum_{n=0}^{\infty}(n+1)^{3/2}\left|J_{n+1}(R)\right| \leq \sqrt{\frac{3}{\pi}}\,\mathrm{e}^2\left(1+R^{4/3}\right)R.$$

Proof: The first kind n$^{\text{th}}$ order Bessel functions have two classical bounds [7, 14, 10]

$$\begin{aligned} |J_n(R)| &\leq \sqrt{\frac{2}{\pi}}\frac{1}{R^{1/3}} \\ |J_n(R)| &\leq \frac{(R/2)^n}{n!}. \end{aligned} \tag{D13}$$

where in the second one, $\sqrt{\frac{2}{\pi}} > 0.7857\ldots$, the constant derived by Landau [10]. Since these two bounds are always true, we can define $f_n(R)$, a special upper bound for the first kind n^{th} order Bessel function, as

$$|J_n(R)| \leq f_n(R) = \begin{cases} \frac{(R/2)^n}{n!} & \text{for } 0 \leq R < \frac{n}{\mathrm{e}}, \\ \\ \sqrt{\frac{2}{\pi}}\frac{1}{R^{1/3}} & \text{for } R \geq \frac{n}{\mathrm{e}}, \end{cases} \tag{D14}$$

Using this equation, we have

$$\begin{aligned} \sum_{n=0}^{\infty}(n+1)^{3/2}\left|J_{n+1}(R)\right| &\leq \sum_{n=1}^{\lfloor \mathrm{e}R \rfloor} n^{3/2}\sqrt{\frac{2}{\pi}}\frac{1}{R^{1/3}} + \sum_{n=\lfloor \mathrm{e}R \rfloor+1}^{\infty} n^{3/2}\frac{(R/2)^n}{n!} \\ &= I_1 + I_2. \end{aligned} \tag{D15}$$

Now we consider each term in the right-hand-side of Eq. (D15) separately. For

the first term we note that for $0 \leq R < \frac{1}{\mathrm{e}}$, we have

$$I_1 = 0. \tag{D16}$$

Now, we assume $R \geq \frac{1}{\mathrm{e}}$ and we have

$$\begin{aligned} I_1 &= \sqrt{\frac{2}{\pi}} \frac{1}{R^{1/3}} \sum_{n=1}^{\lfloor \mathrm{e}R \rfloor} n^{3/2} \\ &\leq \sqrt{\frac{2}{\pi}} \frac{1}{R^{1/3}} \int_1^{\mathrm{e}R+1} x^{3/2} dx \\ &= \frac{2\sqrt{2}}{5\sqrt{\pi}} \frac{(\mathrm{e}R+1)^{5/2} - 1}{R^{1/3}} \\ &\leq \frac{2\sqrt{2}}{5\sqrt{\pi}} \frac{1}{R^{1/3}} \mathrm{e}\sqrt{\mathrm{e}} (R)^{4/3} \left[1 + (\mathrm{e}R+2)^{4/3}\right] \\ &= \frac{2\mathrm{e}\sqrt{2\mathrm{e}}}{5\sqrt{\pi}} R \left[1 + (\mathrm{e}R+2)^{4/3}\right]. \end{aligned} \tag{D17}$$

The first inequality follows from the definition of integration. The second inequality follows from $(\mathrm{e}R+1)^{5/2} - 1 \leq \mathrm{e}\sqrt{\mathrm{e}} R^{4/3} \left[1 + (\mathrm{e}R+2)^{4/3}\right]$ for $R \geq \frac{1}{\mathrm{e}}$. Putting together Eqs. (D16) and (D17), we have

$$I_1 \leq \frac{2\mathrm{e}\sqrt{2\mathrm{e}}}{5\sqrt{\pi}} R \left[1 + (\mathrm{e}R+2)^{4/3}\right]. \tag{D18}$$

for all $R \geq 0$. As for I_2 we first consider $R \geq 1$ as

$$
\begin{aligned}
I_2 &= \sum_{n=\lfloor eR\rfloor+1}^{\infty} n^{3/2}\frac{(R/2)^n}{n!} \qquad \text{(D19)}\\
&\le \sum_{n=\lfloor eR\rfloor+1}^{\infty} \frac{(R/2)^n}{(n-2)!}\\
&= \frac{R^2}{4}\sum_{n=\lfloor eR\rfloor-1}^{\infty} \frac{(R/2)^n}{n!}\\
&\le \frac{R^2}{4}\sum_{n=\lfloor eR\rfloor-1}^{\infty} \frac{(R/2)^n}{(\lfloor eR\rfloor-1)!(\lfloor eR\rfloor-1)^{n-(\lfloor eR\rfloor-1)}}\\
&= \frac{R^2(R/2)^{(\lfloor eR\rfloor-1)}}{4(\lfloor eR\rfloor-1)!}\sum_{n=0}^{\infty}\left[\frac{R}{2(\lfloor eR\rfloor-1)}\right]^n\\
&\le \frac{R^2(R/2)^{(\lfloor eR\rfloor-1)}}{4(\lfloor eR\rfloor-1)!}\sum_{n=0}^{\infty}\left(\frac{1}{e-1}\right)^n\\
&= \frac{(e-1)R^2(R/2)^{(\lfloor eR\rfloor-1)}}{4(e-2)(\lfloor eR\rfloor-1)!}\\
&\le \frac{(e-1)R^2\left[\frac{R}{2(\lfloor eR\rfloor-1)}\right]^{\lfloor eR\rfloor-1}}{4(e-2)\sqrt{2\pi(\lfloor eR\rfloor-1)}}\\
&\le \frac{(e-1)R^{3/2}\left(\frac{1}{e-1}\right)^{\lfloor eR\rfloor-1}}{4(e-2)\sqrt{2\pi}}\sqrt{\frac{2}{e-1}}\\
&= \frac{\sqrt{e-1}R^{3/2}\left(\frac{1}{e-1}\right)^{\lfloor eR\rfloor-1}}{4(e-2)\sqrt{\pi}}\\
&\le \frac{\sqrt{e-1}R^{3/2}\left(\frac{1}{e-1}\right)^{eR-1}}{4(e-2)\sqrt{\pi}}\\
&\le \frac{(e-1)\sqrt{e-1}R}{4(e-2)\sqrt{\pi}}\\
&\le \frac{e-1}{2\sqrt{\pi}(e-2)}R.
\end{aligned}
$$

The first inequality follows from $n^{3/2} \le n(n-1)$ for $n \ge 3$. The second inequality follows from $n! \ge (\lfloor eR\rfloor-1)!(\lfloor eR\rfloor-1)^{n-(\lfloor eR\rfloor-1)}$. In the third and fifth inequality we have used $\frac{R}{2(\lfloor eR\rfloor-1)} \le \frac{1}{e-1}$ for $R \ge 1$. In the fourth inequality, we have applied the

following lower bound to $(\lfloor eR \rfloor - 1)!$, based on Stirling's approximation:

$$\sqrt{2\pi}(\lfloor eR \rfloor - 1)^{\lfloor eR \rfloor - 1 + 0.5} \exp\left[-(\lfloor eR \rfloor - 1)\right] \leq (\lfloor eR \rfloor - 1)!$$

In the fifth inequality we have also used $\sqrt{\frac{R}{2(\lfloor eR \rfloor - 1)}} \leq \sqrt{\frac{2}{e-1}}$ for $R \geq 1$. In the sixth inequality we have used $x \geq \lfloor x \rfloor$ for all x. The seventh inequality follows from $\sqrt{R} \geq (e-1)^{eR}$ for $R \geq 1$.

In a similar way, it could be shown that the bound for I_2 in Eq. (D19) holds for $0 \leq R < 1$ too. Now by combining Eqs (D15), (D18) and (D19) together, we have

$$\begin{aligned}
\sum_{n=0}^{\infty}(n+1)^{3/2}\left|J_{n+1}(R)\right| &\leq \frac{2e\sqrt{2e}}{5\sqrt{\pi}}R\left[1+(eR+2)^{4/3}\right] + \frac{e-1}{2\sqrt{\pi}(e-2)}R \quad \text{(D20)} \\
&= \frac{R}{\sqrt{\pi}}\left\{\frac{2e\sqrt{2e}}{5}\left[1+(eR+2)^{4/3}\right] + \frac{e-1}{2(e-2)}\right\} \\
&\leq \frac{R}{\sqrt{\pi}}\left[\sqrt{3}e^2\left(1+R^{4/3}\right)\right] \\
&= \sqrt{\frac{3}{\pi}}e^2\left(1+R^{4/3}\right)R.
\end{aligned}$$

□

Before presenting Lemma D4 and proof of Theorem 4.2.1 we will define some relevant parameters. Let A_{nm} be the exact values of coefficients in Eq. (3.1) from Eq. (D21) and let A^*_{nm} be the approximated value of these coefficients from Eq. (4.2) as stated in Eq. (D22).

$$A_{nm} = \frac{n+1}{\pi} \int_0^1 \int_0^{2\pi} e^{\beta_1 \rho^2} \prod_{j=2}^{n_{ab}} f_{L_j,M_j}(\rho,\theta)\, V_n^m(\rho,\theta)\, \rho\, d\rho\, d\theta. \tag{D21}$$

$$A^*_{nm} = \frac{n+1}{\pi} \int_0^1 \int_0^{2\pi} e^{\beta_1 \rho^2} \prod_{j=2}^{n_{ab}} T_{L_j,M_j}(\rho,\theta)\, V_n^m(\rho,\theta)\, \rho\, d\rho\, d\theta. \tag{D22}$$

Also let $f_{L_j,M_j}(\rho,\theta)$, $T_{L_j,M_j}(\rho,\theta)$ and $\epsilon_{L_j,M_j}(\rho,\theta)$ be short form expression of the exponential factor of the aberration (L_j, M_j), $\exp\left[\beta_j \rho^{2L_j+M_j} \cos^{M_j}(\theta-\phi_0)\right]$, the Taylor expansion of this exponential expression and the error of this expansion corresponding to the first $N_j{}^*$ terms of the expansion respectively. Also let

$$\begin{aligned} \hat{h}(x,y;x_0,y_0) &= \sum_{n=0}^{\infty} \sum_{m=1}^{n} \tilde{\delta}_{n-m} \delta_m A_{nm} \cos[(\Theta+\phi_0)] \frac{J_{n+1}(R)}{R}, \\ \hat{h}_{n^*}(x,y;x_0,y_0) &= \sum_{n=0}^{n^*} \sum_{m=1}^{n} \tilde{\delta}_{n-m} \delta_m A^*_{nm} \cos[(\Theta+\phi_0)] \frac{J_{n+1}(R)}{R}, \end{aligned} \tag{D23}$$

be the normalized exact and approximated PSF respectively. There, δ_m is one if $m = 0$ and it is two otherwise and $\tilde{\delta}_i$ is one when i is even and it is zero otherwise. We recall that $\hat{h}(x,y;x_0,y_0)$ in Eq. (D23) is the exact PSF and $\hat{h}_{n^*}(x,y;x_0,y_0)$ is the approximate PSF whose accuracy is under investigation.

Let R^* be the radius of the region of interest (exit window) and let n_{ab} be the number of aberrations present in an optical system. We will prove that to have an arbitrarily accurate result in this region we only need a minimum necessary index of summation, n^*, in Eq. (D23) and a minimum necessary number of terms of Taylor expansion for each aberration, $N_j{}^*$, in Eq. (D22). Note that both summation indices

are independent of the value of defocus.

Lemma D4. *Let us assume we have finitely many aberrations (n_{ab}) in an optical system. If*

$$f_{L_j,M_j}(\rho,\theta) - T_{L_j,M_j}(\rho,\theta) = -\epsilon_{L_j,M_j}(\rho,\theta) f_{L_j,M_j}(\rho,\theta), \tag{D24}$$

and

$$N_j{}^* = \max\left(4,\ 2\mathrm{e}\,|\beta_j| + 1,\ \log_2 \frac{\mathrm{e}}{(2\mathrm{e}-1)\sqrt{2\pi\epsilon}}\right). \tag{D25}$$

for all $j = 2 \ldots n_{ab}$ in the system. Then we have

$$\left|\epsilon_{L_j,M_j}\right| \leq \epsilon.$$

for all $j = 2 \ldots n_{ab}$.

Proof: By referring to Eq. (D24), we set $p^* = N_j^*$, $b = \beta_j \cos^{M_j}(\theta - \phi_0)$, $x = \rho$ and $m = 2L_j + M_j$ we can rewrite Eq. (D25) to get

$$p^* = \max\left(4,\ 2\mathrm{e}\,|b| + 1,\ \log_2 \frac{\mathrm{e}}{(2\mathrm{e}-1)\sqrt{2\pi\epsilon}}\right). \tag{D26}$$

Now using Lemma D2, we have

$$\left|f_{L_j,M_j}(\rho,\theta) - T_{L_j,M_j}(\rho,\theta)\right| \leq \epsilon \left|f_{L_j,M_j}(\rho,\theta)\right|. \tag{D27}$$

Substituting the left-hand-side from Eq. (D24), we have

$$\left|\epsilon_{L_j,M_j}(\rho,\theta) f_{L_j,M_j}(\rho,\theta)\right| \leq \epsilon \left|f_{L_j,M_j}(\rho,\theta)\right|. \tag{D28}$$

Simplifying Eq. (D28) yields

$$\left|\epsilon_{L_j,M_j}\right| \leq \epsilon. \tag{D29}$$

□

Proof of Theorem 4.2.1: We first define the error of Taylor expansion, $\epsilon_{L,M}(\rho,\theta)$, as in Lemma D4

$$\epsilon_{L_j,M_j}(\rho,\theta) = \frac{T_{L_j,M_j}(\rho,\theta) - f_{L_j,M_j}(\rho,\theta)}{f_{L_j,M_j}(\rho,\theta)}. \tag{D30}$$

Using the definition of A_{nm} and A^*_{nm} we have (from here on for the sake of simplicity we will not write the dependence of $f_{L,M}$, $T_{L,M}$, $\epsilon_{L,M}$ and V on ρ and θ explicitly)

$$
\begin{aligned}
A_{nm} - A^*_{nm} &= \frac{n+1}{\pi} \int_0^1 \int_0^{2\pi} \left(\prod_{j=2}^{n_{ab}} f_{L_j,M_j} - \prod_{j=2}^{n_{ab}} T_{L_j,M_j} \right) \mathrm{e}^{\beta_1 \rho^2} V_n^m \, \rho \, d\rho \, d\theta \qquad \text{(D31)} \\
&= \frac{n+1}{\pi} \int_0^1 \int_0^{2\pi} \left[\prod_{j=2}^{n_{ab}} f_{L_j,M_j} - \prod_{j=2}^{n_{ab}} f_{L_j,M_j} (1 + \epsilon_{L_j,M_j}) \right] \mathrm{e}^{\beta_1 \rho^2} V_n^m \, \rho \, d\rho \, d\theta \\
&= \frac{n+1}{\pi} \int_0^1 \int_0^{2\pi} \left[\left(\prod_{j=2}^{n_{ab}} f_{L_j,M_j} \right) g \right] \mathrm{e}^{\beta_1 \rho^2} V_n^m \, \rho \, d\rho \, d\theta
\end{aligned}
$$

In the second equality we have used Eq. (D30). The third equality follows from the definition of g in Eq. (D32).

$$
\begin{aligned}
g &= 1 - \prod_{j=2}^{n_{ab}} (1 + \epsilon_{L_j,M_j}) \qquad \text{(D32)} \\
&= \sum_{j=2}^{n_{ab}} \epsilon_{L_j,M_j} + \sum_{j,k=2}^{n_{ab}} \epsilon_{L_j,M_j} \epsilon_{L_k,M_k} + \cdots + \prod_{j=2}^{n_{ab}} \epsilon_{L_j,M_j}.
\end{aligned}
$$

Taking absolute values, we have

$$
\begin{aligned}
|g| &\leq \left|\sum_{j=2}^{n_{ab}} \epsilon_{L_j,M_j}\right| + \left|\sum_{j,k=2}^{n_{ab}} \epsilon_{L_j,M_j}\epsilon_{L_k,M_k}\right| + \cdots + \left|\prod_{j=2}^{n_{ab}} \epsilon_{L_j,M_j}\right| \qquad \text{(D33)} \\
&\leq \binom{n_{ab}-1}{1}\epsilon^{'} + \binom{n_{ab}-1}{2}\epsilon^{'2} + \cdots + \binom{n_{ab}-1}{n_{ab}-1}\epsilon^{'n_{ab}-1} \\
&\leq \binom{n_{ab}}{1}\epsilon^{'} + \binom{n_{ab}}{2}\epsilon^{'2} + \cdots + \binom{n_{ab}}{n_{ab}}\epsilon^{'n_{ab}} \\
&\leq n_{ab}\epsilon^{'}\left(1 + \frac{(1/2)^2}{2!} + \cdots + \frac{(1/2)^{n_{ab}}}{n_{ab}!}\right) \\
&\leq n_{ab}\epsilon^{'}\sum_{j=0}^{\infty}\frac{(1/2)^j}{j!} \\
&= n_{ab}\epsilon^{'}\sqrt{e}
\end{aligned}
$$

The second inequality follows from applying the Lemma D4 by setting

$$
\epsilon^{'} = \frac{\sqrt{\pi}}{2\sqrt{3\mathrm{e}}\,\mathrm{e}^2\, n_{ab}(1+R^{*4/3})}\,\epsilon, \qquad \text{(D34)}
$$

as the desired accuracy. Note that the N_j^* required for this accuracy is precisely what is stated in the expression of Theorem 4.2.1. The fourth inequality follows from $n_{ab}\epsilon^{'} \leq \frac{1}{2}$ (This follows from Eq. (D34) by considering the facts that $\epsilon \leq 1$ and $R^* \geq 0$). Now, taking absolute values in Eq. (D31), we have

$$
\begin{aligned}
|A_{nm} - A^*_{nm}| &\leq \frac{n+1}{\pi} \int_0^1 \int_0^{2\pi} |g|\, |R_n^m(\rho)|\, \rho\, d\rho\, d\theta \qquad \text{(D35)} \\
&\leq \frac{n_{ab}\epsilon^{'}\sqrt{\mathrm{e}}(n+1)}{\pi} \int_0^1 \int_0^{2\pi} |R_n^m(\rho)|\, \rho\, d\rho\, d\theta \\
&= 2n_{ab}\epsilon^{'}\sqrt{\mathrm{e}}(n+1) \int_0^1 |R_n^m(\rho)|\, \rho\, d\rho\, d\theta \\
&\leq 2n_{ab}\epsilon^{'}\sqrt{\mathrm{e}}(n+1)\frac{1}{2\sqrt{n+1}} \\
&= n_{ab}\epsilon^{'}\sqrt{\mathrm{e}}\sqrt{n+1}.
\end{aligned}
$$

The second inequality follows from Eq. (D33). The third inequality follows from Eq. (D7) in Lemma D1. Now using the definition of the normalized exact and approximated PSF in Eq. (D23), we have

$$
\begin{aligned}
\hat{h}(x,y;x_0,y_0) - \hat{h}_{n^*}(x,y;x_0,y_0) = \qquad \text{(D36)} \\
\sum_{n=0}^{n^*} \sum_{m=0}^{n} \delta_m \tilde{\delta}_{n-m} \left(A_{nm} - A^*_{nm}\right) \cos\left[m(\Theta + \phi_0)\right] \frac{J_{n+1}(R)}{R} \\
+ \sum_{n=n^*+1}^{\infty} \sum_{m=0}^{n} \delta_m \tilde{\delta}_{n-m} A_{nm} \cos\left[m(\Theta + \phi_0)\right] \frac{J_{n+1}(R)}{R}.
\end{aligned}
$$

Taking absolute values, we have

$$
\begin{aligned}
&\left|\hat{h}(x,y;x_0,y_0) - \hat{h}_{n^*}(x,y;x_0,y_0)\right| \leq \qquad \text{(D37)}\\
&\left|\sum_{n=0}^{n^*}\sum_{m=0}^{n}\delta_m\tilde{\delta}_{n-m}\left(A_{nm}-A^*_{nm}\right)\cos\left[m(\Theta+\phi_0)\right]\frac{J_{n+1}(R)}{R}\right|\\
&+\left|\sum_{n=n^*+1}^{\infty}\sum_{m=0}^{n}\delta_m\tilde{\delta}_{n-m}A_{nm}\cos\left[m(\Theta+\phi_0)\right]\frac{J_{n+1}(R)}{R}\right|\\
=\;& I_1 + I_2.
\end{aligned}
$$

Now we analyze each part of the right-hand-side of Eq. (D37). After rearranging, the first term, I_1, simplifies to

$$
\begin{aligned}
I_1 &\leq \sum_{n=0}^{n^*}\sum_{m=0}^{n}\delta_m\tilde{\delta}_{n-m}\left|A_{nm}-A^*_{nm}\right|\left|\frac{J_{n+1}(R)}{R}\right| \qquad \text{(D38)}\\
&\leq \sum_{n=0}^{n^*}\sum_{m=0}^{n}\delta_m\tilde{\delta}_{n-m}n_{ab}\epsilon'\sqrt{\mathrm{e}}\sqrt{n+1}\left|\frac{J_{n+1}(R)}{R}\right|\\
&= n_{ab}\epsilon'\sqrt{\mathrm{e}}\sum_{n=0}^{n^*}(n+1)^{3/2}\left|\frac{J_{n+1}(R)}{R}\right|\\
&= \frac{n_{ab}\epsilon'\sqrt{\mathrm{e}}}{R}\sum_{n=0}^{n^*}(n+1)^{3/2}\left|J_{n+1}(R)\right|\\
&\leq \frac{n_{ab}\epsilon'\sqrt{\mathrm{e}}}{R}\sqrt{\frac{3}{\pi}}\,\mathrm{e}^2\left(1+R^{4/3}\right)R\\
&= \frac{n_{ab}\epsilon'\mathrm{e}^2\sqrt{3\mathrm{e}}}{\sqrt{\pi}}\left(1+R^{4/3}\right)\\
&\leq \frac{n_{ab}\epsilon'\mathrm{e}^2\sqrt{3\mathrm{e}}}{\sqrt{\pi}}\left(1+R^{*4/3}\right)\\
&= \frac{\epsilon}{2}.
\end{aligned}
$$

The second inequality follows from Eq. (D35). The third inequality follows from

Lemma D3. The fourth inequality follows from $R \leq R^*$. The last equality follows from Eq. (D34).

By considering the fact that $n - m$ is always even in Zernike polynomials (Note that this has been transferred to Eq. (D37) through the definition of $\tilde{\delta}_{n-m}$), we can further simplify the summation over m in I_2 in Eq. (D37) to get

$$I_2 \leq \sum_{n=n^*+1}^{\infty} \left[\sqrt{n+1} \left| \frac{J_{n+1}(R)}{R} \right| \left(\tilde{\delta}_n + 2 \sum_{m=1}^{n} \tilde{\delta}_{n-m} |\cos[m(\Theta + \phi_0)]| \right) \right] . \quad \text{(D39)}$$

We can further simplify Eq. (D39) to get

$$I_2 \leq \sum_{n=n^*+1}^{\infty} \left[(n+1)^{\frac{3}{2}} \left| \frac{J_{n+1}(R)}{R} \right| \right] . \quad \text{(D40)}$$

Now we can use Eq. (3.5) in Lemma D3 to get

$$I_2 \leq \sum_{n=n^*+1}^{\infty} \left[(n+1)^{\frac{3}{2}} \frac{1}{2n!} \left(\frac{R}{2} \right)^{n-1} \right] . \quad \text{(D41)}$$

Since for $n \geq 5$ we have $n(n-1) > (n+1)^{\frac{3}{2}}$, we can rewrite Eq. (D41) as

$$I_2 \leq \frac{R}{4} \sum_{n=n^*-1}^{\infty} \left[\frac{1}{n!} \left(\frac{R}{2} \right)^{n} \right] . \quad \text{(D42)}$$

From Eq. (D42), it is clear that the right-hand-side reaches its maximum, when $R = R^*$. Thus

$$
\begin{aligned}
I_2 &\leq \frac{R^*}{4} \sum_{n=n^*-1}^{\infty} \left[\frac{1}{n!} \left(\frac{R^*}{2} \right)^n \right] \qquad \text{(D43)} \\
&\leq \frac{R^*}{4} \sum_{n=n^*-1}^{\infty} \frac{\left(\frac{R^*}{2}\right)^n}{(n^*-1)!(n^*-1)^{n-(n^*-1)}} \\
&= \frac{R^*}{4} \frac{\left(\frac{R^*}{2}\right)^{n^*-1}}{(n^*-1)!} \sum_{n=0}^{\infty} \left(\frac{R^*}{2(n^*-1)} \right)^n \\
&\leq \frac{R^*}{4} \frac{\left(\frac{R^*}{2}\right)^{n^*-1}}{(n^*-1)!} \sum_{n=0}^{\infty} \left(\frac{1}{2\mathrm{e}} \right)^n \\
&= \frac{\mathrm{e}R^*}{2(2\mathrm{e}-1)} \frac{\left(\frac{R^*}{2}\right)^{n^*-1}}{(n^*-1)!} \\
&\leq \frac{n^*-1}{2(2\mathrm{e}-1)} \frac{\left(\frac{R^*}{2}\right)^{n^*-1}}{(n^*-1)!} \\
&\leq \frac{n^*-1}{2\mathrm{e}(2\mathrm{e}-1)} \frac{\left(\frac{\mathrm{e}R^*}{2(n^*-1)}\right)^{n^*-1}}{\sqrt{2\pi(n^*-1)}} \\
&\leq \frac{\sqrt{n^*-1}}{2\mathrm{e}(2\mathrm{e}-1)} \frac{\frac{1}{2^{n^*-1}}}{\sqrt{2\pi}} \\
&\leq \frac{1}{2\mathrm{e}(2\mathrm{e}-1)\sqrt{2\pi}} \frac{1}{2^{\frac{n^*-1}{2}}} \\
&\leq \frac{\epsilon}{2}.
\end{aligned}
$$

The second inequality follows from $(n-1)! \geq (n^*-1)!(n^*-1)^{n-(n^*-1)}$. The third and forth inequalities follow from $n^* \geq \mathrm{e}R^* + 1$. In the fifth inequality, we have applied the following lower bound to $(n^*-1)!$, based on Stirling's approximation:

$$\sqrt{2\pi}(n^*-1)^{n^*-1+0.5} \exp\left(-n^*+1\right) < (n^*-1)!.$$

In the sixth inequality, we have used $n^* - 1 \geq \mathrm{e}R^*$. In the seventh inequality, we have used $\sqrt{n} \leq 2^{0.5n}$ for all n. In the eighth inequality, we have used $n^* \geq 2\log_2 \frac{2}{2\mathrm{e}(2\mathrm{e}-1)\sqrt{\pi}\epsilon}$.

Substituting from Eqs. (D38) and (D43) in Eq. (D37), we have

$$\left|\hat{h}(x, y; x_0, y_0) - \hat{h}_{n^*}(x, y; x_0, y_0)\right| \leq \epsilon. \tag{D44}$$

□

Bibliography

[1] S. Bagheri, P. E. X. Silveira, R. Narayanswamy, and D. P. de Farias. Analytical optimal solution of the extension of the depth of field using cubic phase wavefront coding. Under preparation.

[2] M. Born and E. Wolf. *Principles of Optics.* Cambridge University Press, UK, 1992.

[3] J. Braat, P. Dirksen, and A. J. E. M. Janssen. Assessment of an extended nijboer-zernike approach for the computation of optical point-spread-functions. *J. Opt. Soc. Am. A*, 19:858–870, 2002.

[4] J. Braat, P. Dirksen, A. J. E. M. Janssen, and A. S. van de Nes. Extended nijboer-zernike representation of the vector field in the focal region of aberrated high-aperture optical system. *J. Opt. Soc. Am. A*, 20:2281–2292, 2003.

[5] H. A. Buchdahl. *Optical Aberration Coefficients.* Oxford University Press, London, 1958.

[6] W. T. Cathey and E. R. Dowski. New paradigm for imaging systems. *J. App. Opt.*, 41:6080–6092, 2002.

[7] A. Gray and G. B. Mathews. *A Treatise on Bessel Functions and Their Applications to Physics.* Dover Pub. Inc., New York, 1966.

[8] B. H. W. Hendriks, J. J. H. B. Schleipen, S. Stallinga, and H. van Houten. Optical pickup for blue optical recording at na=0.85. *Opt. Rev.*, 6:211–213, 2001.

[9] A. J. E. M. Janssen. Extended nijboer-zernike approach for the computation of optical point-spread functions. *J. Opt. Soc. Am. A*, 19:849–857, 2002.

[10] L. Landau. Monotonicity and bounds on bessel functions. *Mathematical Physics and Quantum Field Theory, Proc. of, H. Warchall, eds.*, 04:147–154, 2000.

[11] R. Narayanswamy, G. E. Johnson, P. E. X. Silveira, and H. B. Wach. Extending the imaging volume for biometric iris recognition. *J. App. Opt.*, 44:701–712, 2005.

[12] C. L. Tranter. *Bessel Functions with Some Physical Applications.* Hart Pub. Co., New York, 1969.

[13] H. B. Urbach and D. A. Bernard. Modeling latent-image formation in the photolithography, using the helmholtz eq. *J. Opt. Soc. Am. A*, 6:1343–1356, 1989.

[14] G. N. Watson. *A Treatise on the Theory of Bessel Functions.* Cambridge University Press, London, 1944.